Fuel 228 (2018) 140–151

Contents lists available at ScienceDirect

Fuel

journal homepage: www.elsevier.com/locate/fuel

Full Length Article

Influence of carbon number of C_1–C_7 hydrocarbons on PAH formation

Hamisu Adamu Dandajeh*, Nicos Ladommatos, Paul Hellier, Aaron Eveleigh

Department of Mechanical Engineering, University College London, Torrington Place, London WC1E 7JE, United Kingdom

ARTICLE INFO

Keywords:
PAHs
Particulates
Carbon number
Hydrocarbons
Pyrolysis

ABSTRACT

The influence of carbon number of seven hydrocarbons (methane, ethane, propane, *n*-butane, i-butane, heptane and toluene) on PAH formation was investigated in a laminar tube reactor. The hydrocarbons underwent oxygen-free pyrolysis within the temperature range of 1050–1350 °C at a fixed carbon concentration of 10,000 ppm on C_1 basis. Particulate and gas phase PAHs were collected at the outlet of the reactor at pyrolysis temperature intervals of 100 °C. The particulates generated were characterised at sub-micron levels in terms of size, number and mass using a differential mobility spectrometer (DMS-500). PAHs from both the gas and particulate samples were extracted using an accelerated solvent extractor (ASE) and the extracts analysed using gas chromatography coupled to mass spectrometry (GCMS). The PAHs studied were the US EPA 16 priority PAHs with particular attention given to group B2, which are possible human carcinogens. The experimental results showed that increase in temperature of the reactor from 1050 to 1350 °C decreased the total PAH concentrations regardless of the carbon number of the hydrocarbon investigated. Increasing the carbon number of C_1–C_7 hydrocarbons decreased the gas phase (GP) PAH concentrations at a temperature of 1350 °C, while the particulate phase (PP) PAH concentrations (as well as those of Group B2 PAHs) decreased at a temperature of 1150 °C. There was increasing and decreasing trends of total PAH concentrations with increasing carbon number of the hydrocarbons at temperatures of 1050 °C and 1350 °C respectively. Benzenoid and five-membered ring PAHs of 2–4 rings were detected in roughly similar concentrations irrespective of the carbon number of the hydrocarbon. Soot propensities, abundance of particle phase PAHs and carcinogenicity of soot particles increased substantially at a temperature of 1050 °C due to isomerisation in the case of the C_4 hydrocarbons and aromatisation in the case of C_7 hydrocarbons. PAHs from toluene and propane had the highest weighted carcinogenicities at a temperature of 1050 °C per unit volume of gas and per unit soot mass respectively. The weighted carcinogenicity (soot mass basis) decreased with increasing carbon number at temperature of 1150 °C. Potential implication of these observations is that hydrocarbons known to produce substantial particulate mass in combustion systems such as an internal combustion engines, could also have low toxicity.

1. Introduction

Atmospheric air quality is continually degraded by particulate emissions from different combustion sources, and stringent global particulate legislation has largely been enacted due to the adverse health effects of these emissions [1]. Understanding particulate production requires detailed knowledge of the formation and growth of particulate molecular precursors. Such understanding can aid the design of particulate controls in practical combustion systems [2].

Polycyclic aromatic hydrocarbons (PAHs), known for some time as major particulate precursors [3], have received substantial attention in the last few decades due to their toxicity [4]. However, PAH formation mechanisms and in particular, effects of fuel composition on PAHs, are yet not fully understood, despite a considerable volume of experimental, theoretical and numerical studies published in the literature [1,3–5].

Evolution of PAHs often begins with the formation of first aromatic ring (phenyl or benzene) via several reaction pathways [1,7,8]. Polyaromatic growth beyond the first ring was initially known to be dominated by the hydrogen-abstraction-acetylene-addition (HACA) mechanism [8], but further studies have established that the HACA mechanism is too slow to explain the observed rates of PAH formation [6]. Additional proposed PAH growth pathways include: methyl-addition and cyclisation [9], phenyl-addition and cyclisation [10], as well as vinyl -addition and cyclisation [11]. Aromatic radical – radical and radical – molecule reactions were also reported [12].

Toxicity of particulate is influenced by the molecular structure of the hydrocarbon [13–16] and the temperature at which the hydrocarbon is burnt [17,18,16]. Hydrocarbons ranging from C_1 to C_7 are used as fuels for such applications as residential heating, gas turbines

* Corresponding author.
E-mail addresses: hamisu.dandajeh.14@ucl.ac.uk, hadandajeh@abu.edu.ng (H.A. Dandajeh).

https://doi.org/10.1016/j.fuel.2018.04.133
Received 6 April 2017; Received in revised form 16 March 2018; Accepted 25 April 2018

and internal combustion engines [13], while they also form principal components of other fuels [19–24]. For example, C_1 to C_2 gases (methane and ethane) are the major components of natural gas. C_3 to C_4 gases (propane and butane) are the main components of liquefied petroleum gas (LPG) [24], while C_4 to C_{12} molecules are the principal components of gasoline [19,23].

Efforts have been made in the literature to study PAH emissions of some hydrocarbons belonging to the range of C_1 to C_7 fuels. For example, C_1 and C_2 fuels [16,25,26]; C_3 and C_4 fuels [16,24,27]; likewise C_7 fuels [13,21,22]. Nevertheless, systematic studies which investigate the influence of increasing carbon number on PAH formation of a homologous series of these fuels are rare. In particular, the influence of carbon number was only investigated in the case of soot formation. For example, in diffusion flame, Ladommatos et al. [28] reported that soot propensity of hydrocarbons molecules increased with carbon number. Crossley et al. [29] proposed a micro-pyrolysis index (MPI) and threshold sooting index (TSI) for a number of hydrocarbons. They reported increase in soot propensity when the carbon number was increased. McEnally and Pfefferle [30] also reported increase in yield sooting index (YSI) for several hydrocarbons when the carbon number was increased.

It is also evident from the foregoing that there are relatively few experimental PAH studies of the individual hydrocarbons in the homologous series of C_1 to C_7 in a tube reactor, and only limited published information is available on particulate characterisation and soot formation in a tube reactor for this homologous series. There is also incomplete information on whether increasing carbon number has an influence on the carcinogenic Group B2 PAHs when they are adsorbed onto soot particles or when they are available in the gas phase.

This paper reports the analysis of particulate and gas phase PAHs of a homologous series of C_1–C_7 hydrocarbons generated in a homogenous tube reactor. The hydrocarbons underwent oxygen free pyrolysis in the temperature range of 1050–1350 °C. The environment and range of temperatures in the reactor resembled, to a degree, the conditions in the core of fuel spray of a diesel engine (oxygen limited zone). PAHs from the particulate and gas phase samples were extracted using an accelerated solvent extraction (ASE) system and the extract was then analysed using gas chromatography coupled with mass spectrometry (GCMS). The PAH studied were the US EPA 16 priority PAHs shown in Table 1, with particular attention being paid to the group B2 PAHs, which are possible human carcinogens.

2. Experimental systems and methods

2.1. Hydrocarbon molecules investigated

Seven, single component hydrocarbon molecules were investigated. This included five single gaseous fuels (methane, ethane, propane, n-butane and i-butane) (BOC UK) and two liquid fuels (heptane and toluene) (Sigma Aldrich, UK). The molecular structures and flow rates of these test fuels are shown in Table 2.

The hydrocarbons listed in Table 2 allowed the following influences of fuel molecular structure to be assessed:

i) Evaluate and confirm the soot propensities of a homologous series of C_1–C_7 hydrocarbons under oxygen free pyrolysis in the tube reactor used for this study
ii) Characterize the soot particles produced from the range of C_1–C_7 hydrocarbons based on size, number and mass using the DMS500 particle size analyser.
iii) Study PAH formation of the C_1–C_7 hydrocarbons
iv) Correlate the soot propensities in (i) with the DMS data in (ii) and the PAH formation data in (iii) above
v) Whether increase in carbon number influences the identity of PAHs formed, and whether they tend to be found in the gas phase (GP) or particle phase (PP), particularly the B2 sub-group PAHs.
vi) Whether hydrocarbons with the same carbon number but different molecular configuration result in altered PAH formation and toxicity of soot particles under pyrolysis conditions.

2.2. Generation of particulate matter and gas phase PAHs

Particulate and gas phase samples were generated in a tube reactor at temperatures ranging from 1050 to 1350 °C under oxygen-free pyrolysis. Fig. 1 shows a schematic of the experimental facility. Nitrogen was used as a carrier gas and was measured at STP conditions using a mass flow controller MFC (1) at a constant flow rate of 20 L/min for all the tests conducted. The flow rates correspond to laminar flow within the reactor (Reynolds number ~200) throughout the temperature range of 1050–1350 °C. The hydrocarbon molecules were injected into the pyrolyser at a fixed carbon flow rate of 10,000 ppm on C_1 basis. Therefore, the volumetric flow rate of methane, as shown in Table 2, was approximately twice as high as that of ethane and three times that of propane. Gaseous hydrocarbon molecules were supplied into the nitrogen stream with the aid of software-controlled solenoid valves. Liquid fuels were first supplied into a vaporiser inlet (2) via a mechanically operated syringe pump prior to mixing with the pre-heated nitrogen.

In order to ensure that the vaporised fuel was mixed homogenously in the pre-heated nitrogen gas, the vaporiser was packed with borosilicate glass beads of 3 mm diameter. The vaporiser was surrounded and heated by an electrical tape heater (RS Components, UK).

The nitrogen gas and the vaporiser were both maintained at a temperature of 150 °C by two separate proportional integral derivative (PID) controllers (RS Components, UK). Another separate PID controller maintained at 120 °C, the soot sampling stainless steel probe (7) leading to the filter housing. This ensured that condensation of gas phase PAHs along the soot sampling probe was avoided.

The combined hydrocarbon/nitrogen stream passed through a heated static mixer (3) which was filled with 8 mm stainless steel ball bearings. The temperature of the static mixer was measured by a type K thermocouple and controlled at > 180 °C. The mixer ensured homogenising of the combined hydrocarbon/nitrogen stream. The alumina tube (Length = 1.44 m, diameter = 0.104 m) was located vertically in an electric furnace. About 0.6 m of the tube length was centrally heated by the electric furnace. The gas residence time was reported previously [16] and was expressed as 4470/T (s), where T (°C) is the temperature of the reactor.

Size and number distributions of soot particles at sub-micron level were determined by a differential mobility spectrometer (Cambustion DMS 500) instrument. Analysis of the particle size distribution was implemented via a sampling probe (6) and a dilution cyclone situated before the DMS 500.

Soot particles were sampled using a stainless-steel probe (7) connected to a vacuum pump. The soot samples were collected on a 70 mm diameter glass micro-fibre filter (Fisher Scientific UK). The filter mass was measured on a high precision mass balance (1 μg resolution) before and after sampling to obtain the mass of soot collected. Gas phase (GP) PAHs were trapped using XAD-2 resin as recommended by the EPA 1999, since it was found to have high trapping and retention efficiencies of PAHs [33]. A glass cartridge filled with 5 g of XAD-2 resin was embedded between two pieces of glass wool and held in a custom-made stainless-steel cartridge. The cartridge was positioned in series after the particulate filter.

The cumulative gas volume (V_g) that passed through the filter and the resin was measured by a diaphragm volumetric gas meter (Bell flow Systems, UK). Soot and gaseous PAH sampling duration was maintained at 15 min for all test conditions. Table 5 shows, at each temperature, the mass of soot (M_s) collected and calculated soot mass concentrations (M_s/V_g) for the C_1–C_7 hydrocarbons. Repeatability checks were conducted during 4 different test periods with ethane as the control hydrocarbon. This was done to detect any daily drift in the experimental

Table 1
List of 16 Priority PAHs and their Carcinogenic groups as classified by US EPA (1993) [31] [32].

Sn	PAHs	PAH Abbreviation	Carcinogenicity Group	Toxicity Factor	Molecular Weight (g/mole)	Number of Rings	Structure
1	Naphthalene	NPH	D	0.001	128	2	
2	Acenaphthylene	ACY	D	0.001	152	3	
3	Acenaphthene	ACN	NA	0.001	154	3	
4	Fluorene	FLU	D	0.001	166	3	
5	Phenanthrene	PHN	D	0.001	178	3	
6	Anthracene	ATR	D	0.01	178	3	
7	Fluoranthene	FLT	D	0.001	202	4	
8	Pyrene	PYR	NA	0.001	202	4	
9	Benzo[a]anthracene	B[a]A	B2	0.1	228	4	
10	Chrysene	CRY	B2	0.01	228	4	
11	Benzo[b]Fluoranthene	B[b]F	B2	0.1	252	5	
12	Benzo[k]Fluoranthene	B[k]F	B2	0.1	252	5	
13	Benzo(a)pyrene	B[a]P	B2	1.0	252	5	
14	Indeno[1,2,3-cd]pyrene	I[123 cd]P	B2	0.1	276	6	
15	Dibenzo[a,h]anthracene	D[ah]A	B2	1.0	278	5	
16	Benzo[g,h,i]perylene	B[ghi]P	D	0.01	276	6	

*Group B2 are 'possibly carcinogenic to humans' while Group D are 'unclassifiable as to carcinogenicity'. NA – Not available.

Table 2
Molecular structures and flow rates of the test hydrocarbons.

Sn	Fuel Molecule	Molecular Structure	Nomenclature	C/H	Flow rate (mL/min)
1	Methane	CH_4	C_1	0.250	206
2	Ethane	$H_3C–CH_3$	C_2	0.333	99.80
3	Propane	$H_3C–CH_2–CH_3$	C_3	0.375	69.90
4	*n*-butane	$H_3C–CH_2–CH_2–CH_3$	nC_4	0.400	48.99
5	i-butane	$H_3C–CH_2–CH_2–CH_3$	iC_4	0.400	48.41
6	Heptane	$H_3C–(CH_2)_5–CH_3$	nC_7	0.4375	0.175
7	Toluene	$C_6H_5\ CH_3$	arC_7	0.875	0.127

equipment and instrumentation. The 95% confidence intervals reported in this paper are thus calculated from the standard deviations and mean of these daily repeat tests with ethane'.

These data therefore provided a measure of daily variability in the PAH analysis of the hydrocarbons investigated and the results that will be discussed in Section 3.0 will be subject to these variabilities.

The soot and the gas phase PAH samples were stored in plastic petri dishes and immediately deep-frozen in the dark before subsequent PAH extraction and GCMS analysis. Detailed particulate generation in the tube reactor and sampling procedures have been described previously by Dandajeh et al. [16].

2.3. Sample extraction and solvent evaporation

PAHs from the particulates and XAD-2 resin samples were extracted using an accelerated solvent extractor (ASE), which is an automated process for extracting PAHs rapidly at elevated temperature and pressure. ASE is recommended by the EPA (Method 3545, SW-846, draft update IVA) [34]. The extraction conditions and specifications for the ASE are shown in Table 3. Extraction of each sample was carried out using dichloromethane (DCM) as solvent.

The dichloromethane containing the extracted PAHs was evaporated by bubbling gently a stream of nitrogen through the solvent vial which was situated in a custom-made PID controlled heating mantle. The temperature of the heating mantle was maintained at the boiling point of dichloromethane (~40 °C). The DCM solvent containing the PAHs was initially concentrated from 60 mL down to about 15 mL and later transferred into a graduated tube centrifuge (0–15 mL) (VWR UK), before finally being concentrated further, down to 1 mL.

2.4. GCMS analysis of concentrated PAH extracts

The 1 mL PAH extracts were analysed using gas chromatography coupled to a mass spectrometry (GCMS) (Agilent, UK). The optimised operating parameters and oven temperature programme used for the GC–MS are shown in Table 4. Injection was carried out using an automatic liquid sampler (ALS), injecting 1 μL of the PAH extract in a split-less mode. The MS was single quadruple run in electron ionization (EI) mode. The GC–MS was calibrated using certified QTM PAH Mix Standard as described in Dandajeh et al. [16].

The Standard (Sigma Aldrich, UK) contained all the 16 PAH compounds shown in Table 1. Calibration curves were developed for each of the 16 PAH compounds and their linearities were ≥98%. The unknown target PAHs in the particulate and resin extracts were quantified by selectively monitoring the PAH ions. This was achieved by identifying the target PAHs based on detection of the ions of each PAH and correlating the retention times of the ions with those of the QTM PAH Mix calibration Standards.

3. Results and discussion

3.1. Soot propensities of C_1–C_7 hydrocarbons

Gravimetric filter soot mass concentrations (mg/m^3) obtained from pyrolysis of C_1–C_7 hydrocarbons are shown in Table 5, with ethane data having 95% confidence interval. The table shows that soot mass concentrations for the various hydrocarbons tested increased when the pyrolysis temperature was increased from 1050 to 1350 °C. These result

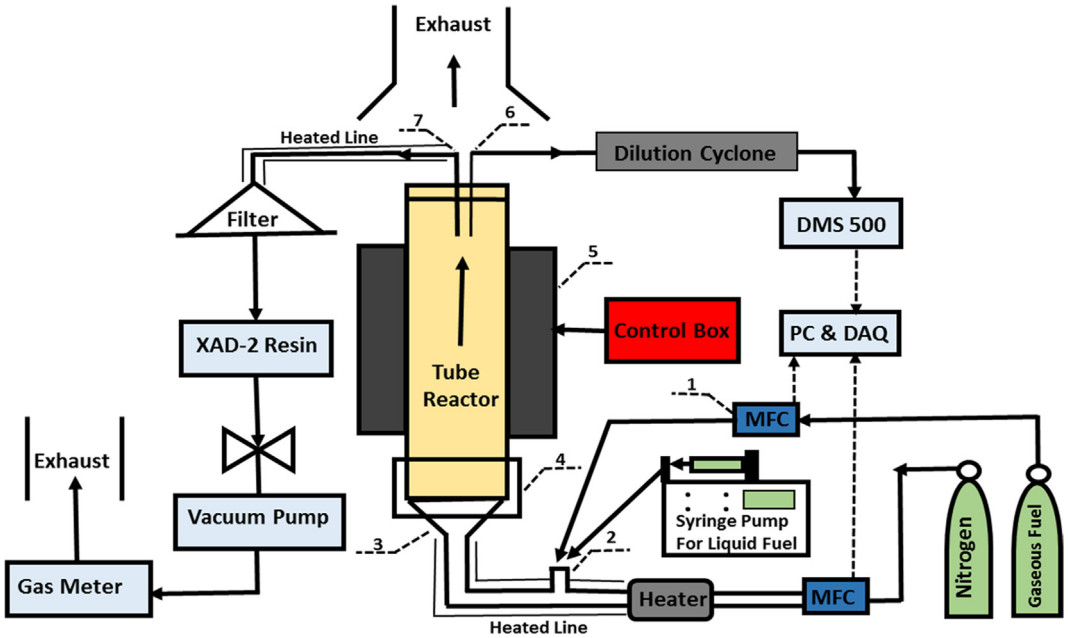

Fig. 1. Schematics of the experimental set-up: 1) mass flow controller (MFC) 2) fuel vaporiser 3) static mixer 4) circulating cooling water 5) tube furnace 6) DMS 500 sampling probe 7) soot sampling probe.

Table 3
Optimised conditions for sample extraction.

Accelerated Solvent Extraction (ASE)	
ASE (Dionex-150, Thermo-Scientific)	
Solvent = Dichloromethane (20 mL)	
Duration for single extraction = 15 min	
Temperature	125 °C
Pressure	1500 bar
Static Cycle	1 (at 5 min)
Extraction Cell	10 mL
Purge Time	60 s
Rinse Volume	40%
Extraction Repeats	3
Final Volume of Extracts	60 mL

Table 4
Optimised conditions for GCMS analysis.

Gas Chromatography Mass Spectrometry (GCMS)		
GC (7890B GC), MSD(5977A)		
Column (HP-5; 30 m × 250 μm × 0.25 μm)		
Total Sample Run Time = 33 min		
Ramp rate (°C/min)	Temperature (°C)	Hold Time (min)
–	50	1
25	150	1
25	200	1
3	230	1
8	310	3

Carrier Gas = Helium at 1.2 L/min, Inlet temperature = 300 °C.
MS Source = 230 °C, MS quad = 150 °C, Transfer line = 290 °C.

match those observed in earlier studies [16,18,35,36]. Methane however stands-out as having zero soot mass concentration at the lowest temperature of 1050 °C. Similar observation was made by Murphy et al. [36], who observed carbon film deposition in methane pyrolysis commencing at temperatures > 1000 °C. As the pyrolysis temperature was raised from 1050 to 1250 °C, the soot mass concentration for methane became unexpectedly high. The high soot concentration of methane at 1250 °C may be influenced by the fact that methane pyrolysis at temperatures of 1200 °C and 1300 °C is dominated by production of

Table 5
Gravimetric filter soot mass concentration of the C1-C7 hydrocarbons.

	Soot Concentration (mg/m^3)			
Temperature(°C)	1050 °C	1150 °C	1250 °C	1350 °C
Methane (C_1)	–	282	1253	1002
Ethane (C_2)	16.0 ± 2.0	434 ± 31.1	956 ± 109	793 ± 77.7
Propane (C_3)	88.2	774	122	966
n-butane (nC_4)	74.6	837	1187	969
i-butane (iC_4)	304	1113	1396	1114
Heptane (nC_7)	20.3	362	727	658
Toluene (arC_7)	745	1300	1379	1286

acetylene and ethylene respectively [37]. Large production rate of acetylene at the temperature of 1250 °C is a likely reason why methane shows slightly higher mass concentration of soot at 1250 °C than those of ethane, propane and *n*-butane, though considerably lower than the concentrations for i-butane and toluene.

As the carbon number of the hydrocarbons was increased from C_1 to C_7, it can be observed from Table 5 that the soot mass concentrations also tended to increase especially at the initial temperature of 1050 °C and it becomes much less apparent as the temperature of the reactor was raised from 1050 to 1350 °C. The correlation coefficient (r) of carbon number as a function of soot mass concentration was only reasonable (r ~ 0.6) at the initial temperature of 1050 °C, suggesting a fairly statistical relationship at this temperature. At the temperature of 1150 °C for example, the soot mass concentration of methane (C_1) was 282 mg/m^3, which then increased by factors of 1.5, 2.6, 3.0, 3.9, 1.3 and 4.6 when C_2, C_3, nC_4, iC_4, nC_7 and arC_7, respectively, were pyrolysed. There was a slight departure from this trend in the mass concentration of heptane (nC_7) for reasons which are not clear, since the pyrolysis of all the fuels was carried out at a fixed carbon concentration. Prior studies in the literature also reported increase in soot propensity of hydrocarbons with increasing carbon number of the fuel [28,31,38], although under flame environments and not always at fixed fuel C_1 supply rates. For example, Ladommatos et al. [28] employed variable flow rates of hydrocarbons in diffusion flames in order to achieve critical sooting heights, from which a similar trend was deduced, that is, an increase in sooting tendency as the carbon number of the fuel was increased.

However, as the pyrolysis temperature of the reactor was increased from 1150 to 1350 °C, there appeared to be less statistical relationship ($r < 0.4$) between the carbon number and soot mass concentration at higher temperatures. Considering now the homologous series of C_1–C_4 hydrocarbons in Table 5, the carbon number and soot mass concentrations at the temperature range of 1050 to 1250 °C are strongly positively correlated ($r > 0.9$), and this correlation appeared to be less ($r = 0.4$) at the highest temperature of 1350 °C. This was evident from the test conditions used in this study, where the flow rate of carbon was kept constant between fuels and there was relatively long residence time ($1.1 \leq t \leq 1.4$) in the absence of oxygen within the reactor. It can also be observed from Table 5 that as the rate of fuel pyrolysis and PAH formation reactions increase with temperature rise, the large difference in soot mass concentration attributable to carbon number between the C_1 to C_7 hydrocarbons was seen to decrease (except heptane).

Comparing the soot propensities of the two C_4 hydrocarbons, Table 5 shows that iC_4 produced a significantly higher soot concentration at the temperature of 1050 °C, by a factor of at least 3 times relative to nC_4, and remained higher at all temperatures. This result is consistent with the studies of Zhang et al. [19], where they reported pyrolysis iC_4 producing more soot mass concentration and higher mass spectrometric signals values of benzene, propargyl and other radicals than the nC_4 over a wide temperature range (550–1550 °C) in a heated flow reactor. The relative difference in soot concentrations for nC_4 and iC_4 decreased when the temperature was increased to 1350 °C. The reason for the increased soot concentration for iC_4 compared with nC_4 is that pyrolysis of iC_4 produces intermediate radicals such as propargyl and C_4 species [39] which are key to the formation of the first aromatic ring, and subsequent growth of PAHs and soot.

Table 5 also shows that the soot concentration of arC_7 at the temperature of 1050 °C is approximately 37 times greater than that for nC_7. This result is in line with those of previous studies [28,38]. The exceptionally high soot concentration of toluene, as an aromatic molecule was expected, since its decomposition produces phenyl and benzyl radicals via self-de-methylation and hydrogen-abstraction respectively [21]. Phenyl radicals are PAH growth species in the phenyl addition and cyclization (PAC) mechanism [10]. Abundance of acetylene in toluene pyrolysis [21] could also accelerate the growth of PAHs and soot surface growth via the HACA mechanism [8].

3.2. Particulate characteristics of C_1–C_7 hydrocarbons

Soot particles produced by pyrolysis of the seven hydrocarbons were characterised in terms of particle mass, size and number concentrations using a differential mobility spectrometer (Cambustion DMS500). The DMS data are summarised in Table 6, with ethane data having 95% confidence interval. The Table presents the influence of temperature on soot particle mean diameter (nm) and total soot particle number concentration (particle number per unit volume of N_2 carrier gas at N_2 inlet conditions). At the temperature of 1050 °C for example, soot particle mean diameter (D_{pm}) of the hydrocarbons increased as their carbon number was increased from C_1 to C_3 and iC_4 to arC_7. However, nC_4 and nC_7 departed to a degree, from this trend. Table 6 shows that there is a shift toward larger soot particles with increasing pyrolysis temperature from 1050 to 1350 °C regardless of the carbon number of the hydrocarbon tested. For example, Dandajeh et al. [40] reported ethane pyrolysis at a temperature of 1050 °C producing particles in the size range of 13–86 nm, whereas at the higher temperature of 1350 °C, particles were broadly distributed in the size range of 86–562 nm. It can also be deduced from Table 6 that particles ranging from 3 to 30 nm, composing of volatile organic compounds, are assumed to be formed from nucleation mechanisms and these particles contain most of the particle number concentrations shown in Table 6. Larger particles were believed to be formed via agglomeration of smaller particles (carbonaceous agglomerates) and condensation of heavy hydrocarbons and these accumulation mode particles contribute to most of the particle mass [41]. It is likely therefore that the soot particle sizes reported in Table 6 were produced during accumulation mode. This can be explained by the fact at the temperature of 1000 °C, for example, the gas residence in the pyrolyser as measured by Eveleigh et al. [42] at nitrogen flow rate of 20 L/min was long (1.4 s) and it shortened to 1.13 s at higher temperature of 1300 °C. It can also be noticeable from Table 6 that at higher temperatures of 1250 and 1350 °C, all the hydrocarbons tested appeared to make particles of roughly the same, suggesting that the soot particle size is independent on temperature.

It can also be observed from Table 6 that, at a temperature of 1050 °C, taking into cognisance the 95% confidence interval, the soot particle sizes produced from pyrolysis of i-butane and toluene are bigger, but the remaining hydrocarbon fuels produced particles that are approximately of the same size. The results at the temperature of 1050 °C suggest a correlation between particle mass and particle diameter, which might make good sense for accumulation mode particles, even if more particles are formed then there is more opportunity for agglomeration. It is also evident from Table 6 that the soot mass concentration is determined by the bigger soot particle sizes of smaller number, than the many smaller particles of smaller sizes. Considering now Table 6 as a whole, it is apparent that as the pyrolysis temperature was increased from 1050 to 1350 °C, the particles became bigger and also the total number of particles become fewer, irrespective of the carbon number of the fuels. It can be concluded therefore that as the temperature rose, the particles agglomerated into fewer larger particles, but with the larger particles still growing, with the result that the total mass of the particles increases. So, while agglomeration produced fewer larger particles, the fewer particles continued to grow through agglomeration but also new soot deposition on them.

As the temperature was increased to 1150 °C, D_{pm} appeared to increase with increasing carbon number of the hydrocarbons, but became almost independent of carbon number at temperature of 1350 °C. This is believed to be due to agglomeration of soot particles which could have resulted in increase in soot particle sizes [43].

Table 6 shows that the soot particle number concentration of all the hydrocarbons decreased when the temperature was increased from 1050 to 1350 °C. It can also be observed from the Table that both iC_4 and nC_4 had nearly the same soot particle number concentration at all the temperatures. Soot particle agglomeration for the C_4 fuels increased with temperature increase at apparently similar rates. These results

Table 6
Soot particle size and number concentration measurements using DMS500.

	Mean Particle Size, D_{pm} (nm)				Number Concentrations (dN/dDp) (1/cm^3)			
Temperature (°C)	1050	1150	1250	1350	1050	1150	1250	1350
Methane (C_1)	38.7	191	381	356	1.8E+7	1.1E+9	2.6E+8	2.2E+8
Ethane (C_2)	40.3 ± 15	223 ± 41	323 ± 55	306 ± 56	2.3E+9 ± 2.6E8	2.8E+8 ± 1.2E8	2.4E+8 ± 6.3E7	3.9E+8 ± 2.6E7
Propane (C_3)	58.0	251	332	362	2.9E+9	8.2E+8	2.9E+8	2.8E++8
n-butane (nC_4)	55.0	247	353	287	2.8E+9	2.5E+8	2.4E+8	5.9E+8
i-butane (iC_4)	90.0	287	379	312	2.8E+9	2.3E+8	2.3E+8	5.2E+8
Heptane (nC_7)	31.0	246	256	304	2.3E+9	2.6E+8	4.2E+8	3.1E+8
Toluene (arC_7)	308	356	410	375	2.3E+8	2.6E+8	2.8E+8	3.4E+8

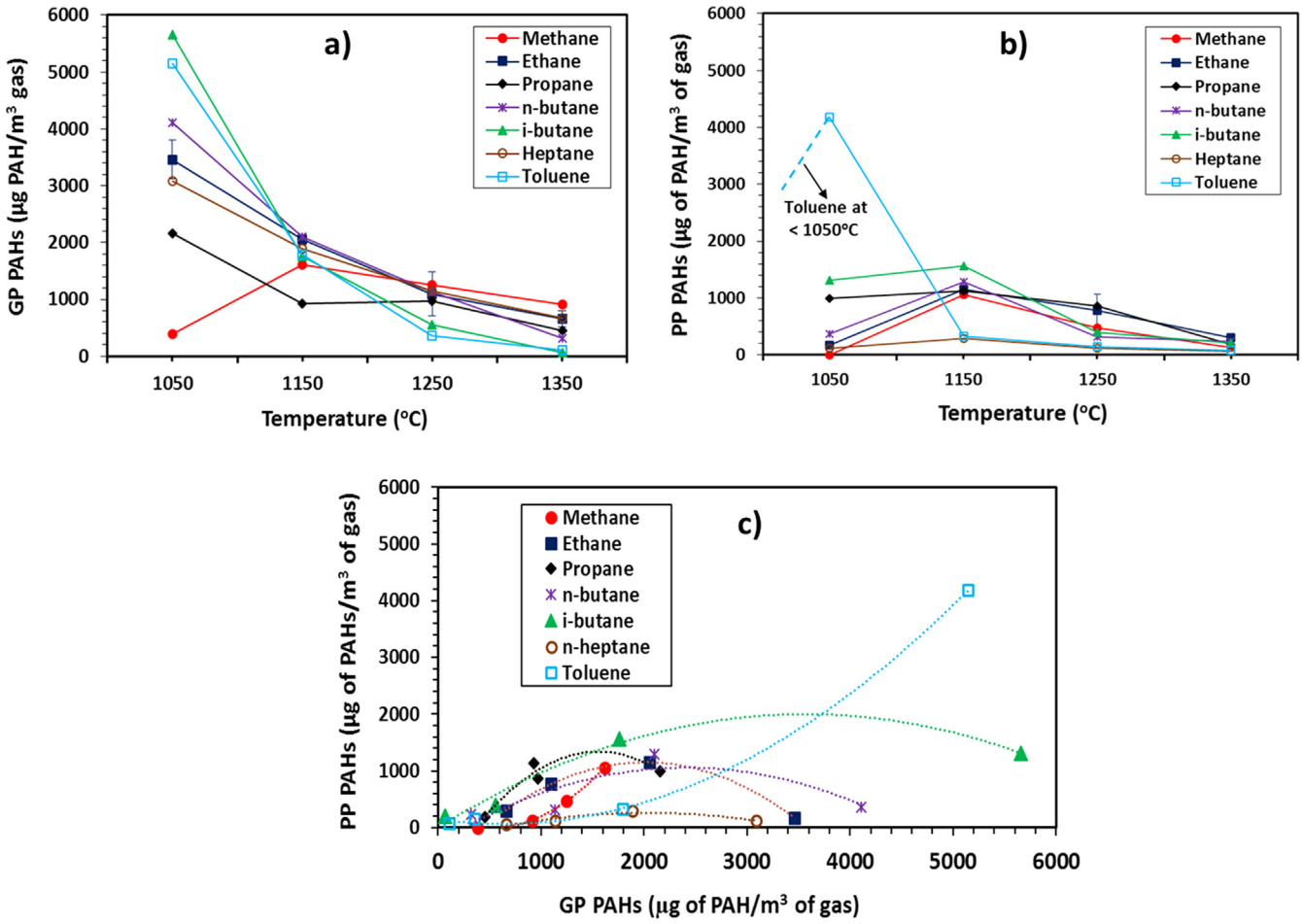

Fig. 2. Normalised Total PAH Concentrations: a) Gas Phase (µg of PAH/m^3 of gas) b) Particle Phase (µg of PAH/m^3 of gas) c) PP and GP at four different temperature points: 1050 °C, 1150 °C, 1250 °C and 1350 °C.

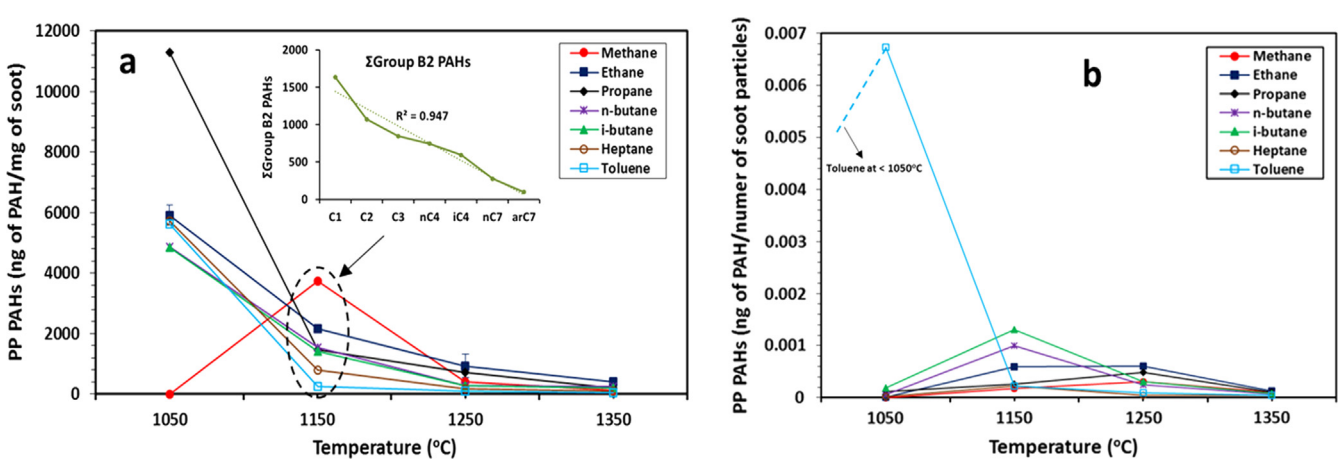

Fig. 3. Normalised Total PAH Concentrations: a) Particle Phase (ng of PAH/mg of soot) b) Particle Phase (µg of PAH/soot particle number).

would seem to suggest that branching a straight chain nC_4 to iC_4 still produces similar number of soot particles, but with considerably larger mean particle size. The variation of soot particle number for nC_7 and arC_7 suggests that the soot particle number for toluene at the four test temperatures are of the same order of magnitude, therefore almost independent of temperature. The mean diameter for toluene at 1050 °C can be seen to be roughly similar to the mean diameter for heptane at 1350 °C. The implication of this observation is that toluene soot particles also appear to grow through agglomeration and by means of deposition of gaseous species on the particles already formed. It is imperative to note that the trends of soot mass concentrations measured using the DMS500 (see Table A1 in Appendix A) agree with those from the gravimetric filter measurements shown in Table 5.

In conclusion, soot formation for the C_1–C_7 hydrocarbons has several common features, with methane and toluene departing somewhat from these common characteristics. Methane had the smallest number of primary particles at 1050 °C, suggesting that reactions were too slow at this temperature for soot formation, compared with most of the other

Table 7
Total PAH (GP + PP) distributions of C_1–C_7 hydrocarbons (μg of PAHs/ m^3 of gas); where 'nd' denotes PAHs that were 'not detected' by the GC.

	1050 °C									1150 °C									1250 °C									1350 °C				
PAHs	C1	C2	C3	nC4	iC4	alC7	arC7	C1	C2	C3	nC4	iC4	alC7	arC7	C1	C2	C3	nC4	iC4	alC7	arC7	C1	C2	C3	nC4	iC4	alC7	arC7
NPH	44.7	1073	210	326	580	220	344	407	204	197	195	189	197	344	278	474	132	116	97.8	209	4.3	277	139	123	107	3.9	196	4.1
ACY	69.3	407	344	342	1294	355	340	421	299	324	244	276	303	340	388	632	265	181	193	297	317	254	259	226	271	117	249	nd
ACN	nd	nd	322	520	8.09	754	11	9.3	1025	7.5	635	702	678	nd	nd	627	nd	492	7.42	305	8.3	nd	nd	nd	nd	nd	nd	nd
FLU	41.8	324	193	255	297	178	397	220	163	138	143	135	172	397	108	252	69	75.9	nd	69.1	nd	nd	69.1	nd	nd	nd	nd	nd
PHN	46.2	191	74.7	133	311	89.3	109	154	97	65.9	83	100	97.6	109	136	219	56	63.3	112	94	51	130	94.5	59.6	94.4	41	91.2	55
ATR	1.07	nd	1.69	640	2.2	1.5	2473	2.5	2.1	2.0	259	1.0	1.92	2473	nd	257	494	nd	81.7	1.9	nd	nd	nd	487	nd	nd	nd	nd
FLT	71.9	228	206	285	1046	170	642	147	218	188	237	241	163	642	158	395	166	141	160	73	53	138	167	160	101	60	74.2	54
PYR	113	360	433	777	384	260	334	430	285	267	322	365	256	334	344	666	244	212	235	104	82	236	178	170	134	120	103	76
B[a]A	0.5	0.45	0.56	0.58	1.02	0.45	180	1.18	0.96	0.95	1.5	1.8	0.89	180	0.54	2.03	0.9	0.51	0.45	0.87	0.5	0.5	0.44	0.94	0.49	0.9	0.86	0.5
CRY	2.19	140	23	361	22.4	196	1043	nd	35.9	29.4	4.5	8.0	36.8	1043	2.38	nd	4.1	2.3	2.0	3.84	nd	nd	nd	4.2	nd	nd	nd	nd
B[b]F	1.75	1.6	1.97	2.06	3.61	1.59	272	4.15	3.4	3.35	5.3	4.66	3.15	272	1.89	7.15	3.2	1.81	1.59	3.055	1.9	1.9	1.56	3.3	1.71	3.3	3.04	1.6
B[k]F	2.3	330	470	496	791	720	1995	258	317	389	442	262	51.1	1995	2.49	444	110	44.8	4.36	24.41	4.9	2.5	2.06	4.36	2.26	4.4	4.01	2.1
B[a]P	5.89	11.5	197	45.6	571	56.2	404	65	58.8	62.5	177	218	20.8	404	42.3	219	127	56.2	28	22.73	13	6.5	5.27	11.1	5.77	11	26.1	12
I[123 cd]P	8.22	190	270	198	348	13.8	161	142	157	178	180	206	33.8	161	27.2	207	28	14.2	7.47	17.11	9.0	9	7.35	15.6	8.05	16	14.3	7.6
D[ah]A	6.65	6.1	95.9	7.84	13.7	6.05	348	15.8	12.9	12.7	20	24.2	12	348	7.21	27.2	12	6.9	6.05	11.64	7.3	7.3	5.95	12.6	6.52	13	11.6	6.1
B[ghi]P	404	383	311	97.1	1320	192	754	337	337	261	476	642	173	754	118	594	162	58.1	44.7	55.19	3.1	70	57	5.33	5.52	5.4	4.91	2.6

C_2–C_7 fuels. Toluene on the other hand had a relatively large mean particle size (308 nm) even at the low temperature of 1050 °C. The particle size for toluene at the lowest temperature of 1050 °C was similar to that for most of the other aliphatic C_1–C_7 hydrocarbons but at the higher temperature of 1350 °C. This implies that of the molecules tested, methane and toluene are at the two extreme ends in terms of soot formation rate, with methane the least and toluene the most prolific soot producer.

3.3. Influence of carbon number on GP and PP PAHs

Fig. 2 presents PAH concentrations of C_1–C_7 hydrocarbons which resulted from summing up, for each hydrocarbon, all the 16 EPA PAHs shown in Table 1. Fig. 2a shows gas phase (GP) PAH mass extracted from the XAD-2 resin and normalised with the volume of gas (V_g) passed through the resin in series with the particulate filter. Fig. 2b shows particulate phase (PP) PAH mass, extracted from the particulates collected on the filter, also normalised with V_g. Fig. 2c shows normalised PP PAH plotted against normalised GP PAHs. Error bars in Fig. 2 denote standard deviations while detailed error bars on the PAH speciation can be found in Dandajeh et al. [7].

It can be seen from Fig. 2a that increasing the temperature of the reactor from 1050 to 1350 °C resulted in lower GP PAH concentrations for all the fuels. This effect of temperature is consistent with other published works [44,16]. Methane was an exception though, with a near zero GP PAH mass at the temperature of 1050 °C. This is likely due to slower formation rates of intermediate precursors (such as acetylene) during methane pyrolysis at 1050 °C. It can also be observed from Fig. 2a, at the temperature of 1350 °C that the GP PAH concentrations decreased with increasing carbon number of the hydrocarbons, but the trend is unclear at other temperatures.

The PP PAH mass concentration shown in Fig. 2b increase within the temperature range of 1050–1150 °C for all the fuels except toluene, but as the temperature was raised further from 1150 to 1350 °C, the PAH concentration subsequently decreased. This decreasing trend of PP PAH concentrations above 1150 °C is believed to be due to incorporation of PP PAHs (particularly Group B2) into soot; and has been reported previously by Aracil et al. [45] in pyrolysis of polyvinylchloride. Comparing Fig. 2a and b at the temperature of 1050 °C shows that both the GP and PP PAHs on volume of gas basis increase with increasing carbon number of the hydrocarbons examined. Although this does not seem to apply in the case of propane and heptane pyrolyses.

Fig. 2c shows the GP and PP PAHs concentrations of the seven hydrocarbons plotted against each other at four different temperatures (1050 °C, 1150 °C, 1250 °C and 1350 °C) and the curves suggest that the abundance of both GP and PP PAHs is influenced by temperature. That is, the abundance of both reduces with temperature and this is possibly due to more rapid conversion of GP to soot (see Table 5). More detailed observation of Fig. 2c shows that the PP PAH concentration increased while GP PAHs increased and this relation held up to the temperature of 1150 °C; as the temperature rose further to 1350 °C, both GP and PP PAH concentration reduced together (methane and toluene are exceptions to this trend). Considering now Fig. 2a, 2b and 2c together, concentration of higher GP and PP PAHs can be observed at the temperature of 1050 °C for iC_4 over nC_4 as well as for arC_7 over nC_7. This observation suggests that isomerisation and aromatisation of the respective C_4 and C_7 fuels at 1050 °C, both promote formation of molecular precursors of soot as well as higher soot concentration and larger soot particle sizes (see Table 5).

PP PAH mass was normalised in two ways, in Fig. 3a by the soot mass (see Table 5) and in Fig. 3b by the soot particle number (see Table 6). Fig. 3a shows that the concentration of PP PAHs per unit mass of soot decreased substantially with increasing temperature of the reactor from 1050 to 1350 °C for all the fuels. That is, a relatively smaller amount of PAHs was deposited on soot particles, per unit mass of soot, while the amount of soot increased as the temperature rose. Fig. 3a

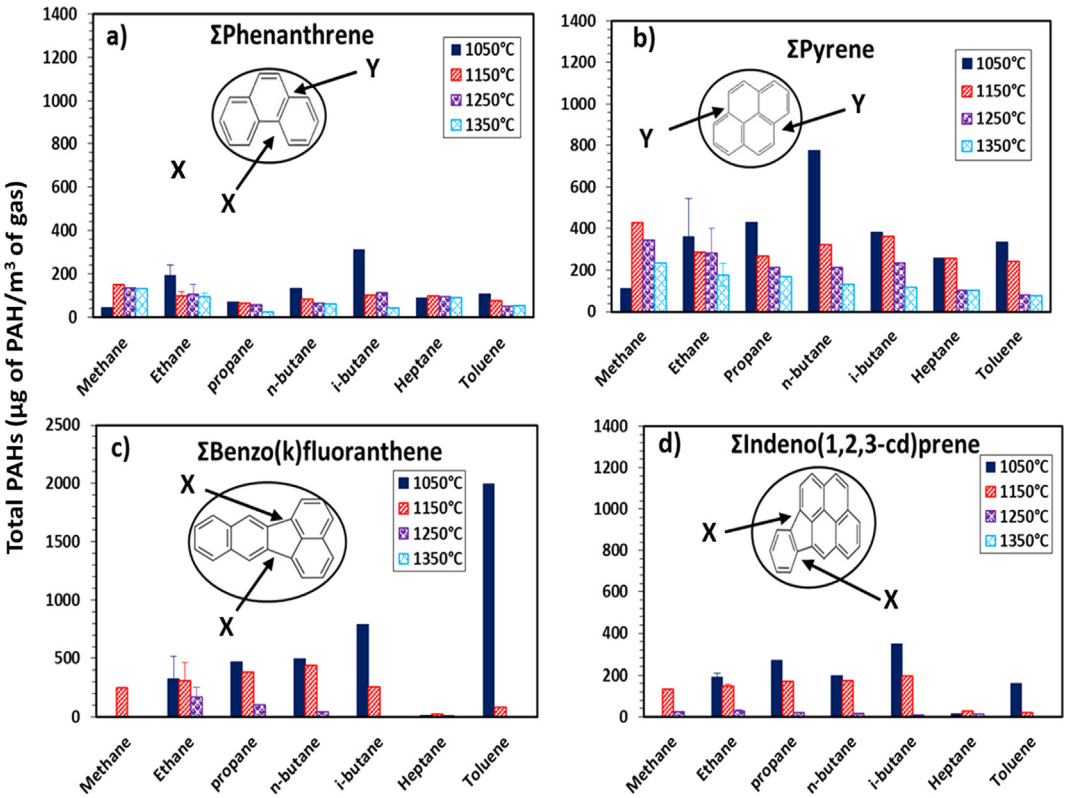

Fig. 4. Distributions of total PAHs produced during the pyrolysis of C_1–C_7 hydrocarbons a) Phenanthrene b) Pyrene c) Benzo(k)fluoranthene d) Indeno(1,2,3-cd) pyrene.

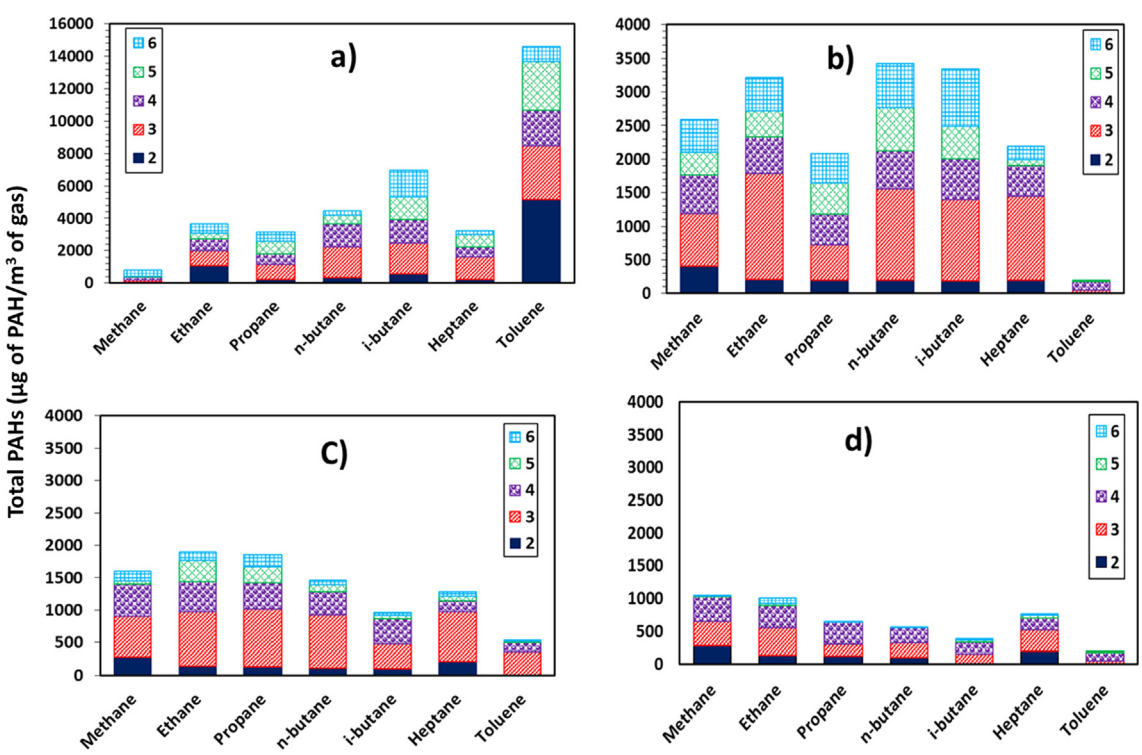

Fig. 5. Total PAH concentrations with respect to their number rings for the C_1–C_7 hydrocarbons at four different temperature points: a) 1050 °C b) 1150 °C c) 1250 °C d) 1350 °C. The legend on the graphs denotes number of PAH rings.

shows that at the temperature of 1150 °C, the PP PAH concentrations (as well as the Group B2 PAH concentration) at a temperature of 1150 °C decreased with increasing carbon number. It can also be seen in Fig. 3a that the PP PAH concentration at a temperature of 1050 °C during methane pyrolysis was zero due to absence of soot at such temperature (see Table 5).

What stands out in Fig. 3b and Fig. 2b is the PP PAH concentration of toluene at a temperature of 1050 °C. Toluene is a source of large

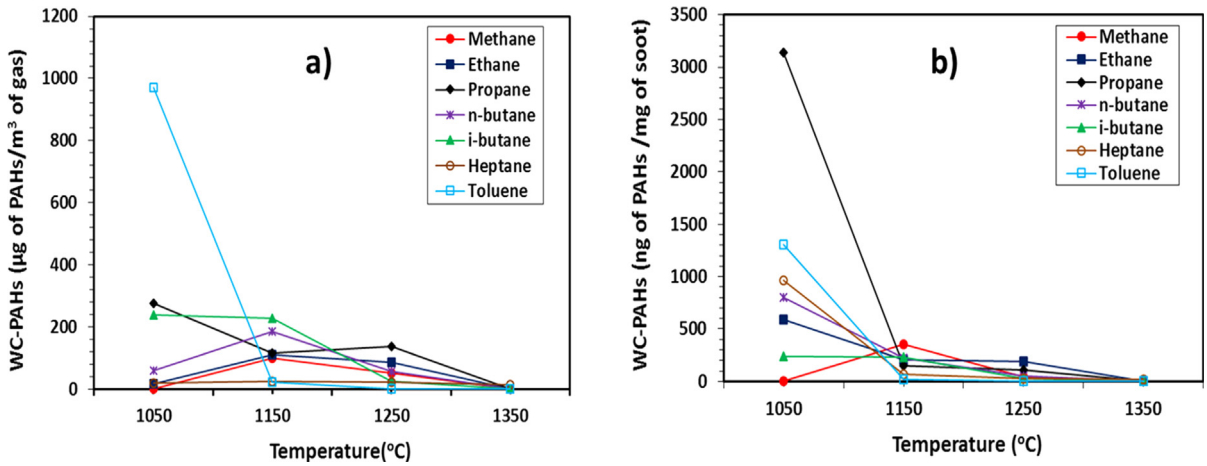

Fig. 6. Normalised Weighted Carcinogenicity: a) weighted carcinogenicity of PP PAHs (µg of PAH/m^3 of gas) b) weighted carcinogenicity of PP PAHs (ng of PAH/ mg of soot).

number of intermediates (phenyl and benzyl radicals) at lower temperatures [10], which can contribute to PAH and soot particle growth. This is reflected by the appreciable soot mass concentrations of toluene at the temperature of 1050 °C relative to the other hydrocarbons examined. It is expected that at temperatures < 1050 °C (see Fig. 3b and Fig. 2b) toluene will exhibit an increasing trend in the PP PAH concentrations with rising temperatures to 1050 °C.

The above extrapolation of toluene PAH mass for temperatures lower than 1050 °C is supported by the findings of other published studies. For example, Sanchez et. al. [44,18] reported increasing trend in PAH concentrations of C_2 fuels within the temperature range of 700–950 °C and a corresponding decrease in PAH mass at temperatures > 950 °C.

Fig. 3a suggests that different structures of hydrocarbons with the same carbon number (nC_4 & iC_4 and nC_7 & arC_7) produced roughly similar PP PAH concentrations per unit mass (M_s) of soot at all temperatures. The PP PAHs normalised with the number of soot particles are shown in Fig. 3b. The concentrations of PAHs per soot particle increased when the pyrolysis temperature was increased from 1050 to 1150 °C and drastically decreased when the temperature was raised to 1350 °C (toluene is still an exception). Fig. 3b shows that hydrocarbons with the same carbon number (nC_4 & iC_4 and nC_7 & arC_7), yielded identical PAH mass within the temperature range of 1250–1350 °C.

3.4. Influence of carbon number on individual total PAHs

This section examines the PAH distribution for individual C_1–C_7 hydrocarbons. Table 7 presents the distributions of the 16 EPA priority PAHs for each hydrocarbon fuel, while Fig. 4a, b, c and d show the PAH concentrations of PHN, PYR, B(k)F and I(1,2,3-cd)P respectively. These four PAHs were selected from Table 7 as examples for further discussion. It can be seen from Fig. 4a and b that lighter benzenoid PAHs (PHN and PYR) were detected in roughly similar concentrations, at all temperatures, regardless of the carbon number of the hydrocarbon. A similar observation can be seen in Table 7 for lighter five-membered ring PAHs (ACY and FLT). Formation of lighter PAHs at low temperatures of 1050 °C was reported to be dominated either by aromatic radical-radical or radical-molecule reactions [12]. For example, kinked PAHs, such as phenanthrene, with one arm chair feature (site X in Fig. 4) could grow to pyrene via reaction of phenanthrene radical and acetylene molecule. However, the growth of pyrene to heavier PAHs was reported to be inefficient through the HACA mechanism [12] due to its multiple double fusing sites (site Y in Fig. 4).

Fig. 4c and d were plotted for the temperature of 1050 °C and show an increasing trend of heavier five membered ring PAHs, B(k)F and I(1,2,3-cd)P, with increasing carbon number of the hydrocarbon. This observation however, does not seem to apply in the case of heptane pyrolysis in Fig. 4c and heptane and toluene pyrolyses in Fig. 4d. On the contrary, Table 7 shows no such clear trend for heavier benzenoid PAHs (B(a)P, D(a,h) and B[ghi]P) at temperature of 1050 °C. It should be noted that five-membered ring PAHs have a common feature of multiple triple fusing sites/arm-chairs, making it easier for PAH growth via the HACA mechanism [10].

One striking characteristic of the heavier PAHs (together with few of the lighter PAHs) shown in Table 7, is their disappearance at the higher temperature of 1350 °C. Smith [46] and Shukla et al. [12] both also reported this observation in the case of toluene pyrolysis. The disappearance of these PAHs at high temperatures has been ascribed to insufficient soot surface area/number of soot particles available for PAH condensation [16].

The soot particle number concentrations of the hydrocarbons shown in Table 6 showed remarkable decrease with temperature increase to 1350 °C. For example, when the pyrolysis temperature was increase from 1050 to 1350 °C, the soot particle number concentrations decreased by factors of ~6, 10, 5, 5 and 7 in the case of the C_2, C_3, nC_4, iC_4 and nC_7 hydrocarbons, respectively. Shukla et al. [12] reported that the kinetics for the formation of heavier PAHs at high temperatures of 1350 °C is dominated by the HACA mechanism.

It is interesting to note that most of the PAHs detected in this paper at high concentrations in the pyrolysis of the individual C_1–C_7 hydrocarbons (see Table 7), were also reported in high concentrations in previous published works [12,21,22,25,26,24,27].

3.5. Effects of carbon number on PAH rings

Fig. 5 shows the concentrations of PAHs in terms of number of rings (size of PAHs) for the seven hydrocarbon fuels. Fig. 5a, b, c and d show the total PAH concentrations at temperatures of 1050 °C, 1150 °C, 1250 °C and 1350 °C respectively. It can be seen from Fig. 5a that concentrations of the total number of PAH rings at a temperature of 1050 °C, particularly those of 3, 4 and 5 rings, increased with increase in carbon number of the hydrocarbons from C_1–C_7, but surprisingly this does not seem to apply in the case of heptane pyrolysis.

It can also be seen from Fig. 5a that pyrolysis of iC_4 produced higher number of 2, 5 and 6 rings compared to the corresponding nC_4. Similarly, Fig. 5a shows that pyrolysis of aromatic toluene (arC_7) produced substantially higher number of 2–6 ring PAHs compared to the aliphatic heptane molecule (nC_7). As the temperature of the reactor was increased from 1150 to 1350 °C, the concentrations of the PAHs decreased, but especially so in the case of the hydrocarbons with larger

Table 8
Particulate Phase (PP) PAH distributions of C_1–C_7 hydrocarbons (ng of PAHs/mg of soot); where 'nd' denotes PAHs that were 'not detected' by the GC.

	1050 °C							1150 °C							1250 °C							1350 °C						
PAHs	C1	C2	C3	nC4	iC4	alC7	arC7	C1	C2	C3	nC4	iC4	alC7	arC7	C1	C2	C3	nC4	iC4	alC7	arC7	C1	C2	C3	C4	iC4	alC7	arC7
NPH	0.0	35.5	26.3	16.2	11	44.04	6.03	10.03	4.05	2.82	6.55	4.95	5.3	1.3	1.8	2.12	1.4	1.8	1.3	2.7	1.5	2.2	2.4	2.1	2.1	1.8	2.8	1.5
ACY	0.0	264	nd	nd	nd	nd	nd	nd	52.1	73.1	nd	nd	nd	nd	nd	61.5	19	nd	10	nd	nd	nd	85	66.1	114	58	nd	nd
ACN	0.0	nd	nd	nd	nd	nd	nd	nd	nd	nd	nd	nd	nd	nd	nd	nd	nd	nd	nd	nd	nd	nd	nd	nd	nd	nd	nd	nd
FLU	0.0	247	nd	nd	nd	nd	nd	nd	nd	nd	nd	nd	nd	nd	nd	nd	nd	nd	nd	nd	nd	nd	nd	nd	nd	nd	nd	nd
PHN	0.0	155	33.77	55.35	47.1	56.55	68.2	12.88	28.9	25.3	22.4	23.7	6.8	1.7	2.3	27.8	19	9.8	2.7	3.4	7.0	21	49	36.8	36	20	3.6	1.9
ATR	0.0	nd	nd	nd	nd	nd	1334	nd	nd	nd	nd	nd	nd	nd	nd	nd	133	nd	59	nd	nd	nd	nd	505	nd	nd	nd	nd
FLT	0.0	367	385.7	209	225	247.6	339	10.51	157	87.8	95.3	88.1	23	20	36	133	79	48	62	10	35	45	116	105	102	1.9	29	19
PYR	0.0	689	826.1	424.1	471	377.3	206	557.9	223	145	133	150	47	33	93	199	120	69	94	2.0	55	55	73	82.5	137	106	36	36
B[a]A	0.0	8.58	6.354	3.912	2.66	10.64	241	2.423	0.98	0.68	1.22	1.2	1.3	0.3	0.4	0.51	0.3	0.4	0.3	0.6	0.4	0.5	0.6	0.51	0.5	0.4	0.7	0.4
CRY	0.0	nd	272.2	79.99	87.8	162.1	279	3.04	71.8	38	1.4	2.3	1.3	3.1	nd	1.1	0.4	1.1	2.0	1.2	2.8	nd	nd	nd	nd	nd	nd	nd
B[b]F	0.0	30.2	22.38	13.78	9.37	37.47	364	8.534	3.45	2.4	4.28	4.21	4.5	1.1	1.5	1.8	1.2	1.5	1.1	2.3	1.3	1.9	2.1	1.78	1.8	1.6	2.4	1.3
B[k]F	0.0	1174	2388	1229	891	1861	1383	904.9	597	500	355	235	135	66	2.0	204	88	38	1.5	31	1.7	2.5	2.7	2.35	2.3	2.0	3.2	1.7
B[a]P	0.0	311	1541	564.2	698	707.1	538	209.4	101	74.2	161	158	43	9.0	34	159	99	42	16	25	4.4	6.4	7	6.02	6	5.2	21	4.2
I[123 cd]P	0.0	1131	2414	1027	735	488.5	211	474.7	283	221	206	178	74	15	22	33.6	16	12	5.4	14	6.2	9	9.7	8.4	8.3	7.3	11	5.9
D[ah]A	0.0	115	1087	52.49	35.7	142.8	462	32.52	13.1	9.15	16.3	16	17	4.3	5.7	6.86	4.4	5.8	4.3	8.7	5.0	7.3	7.9	6.8	6.7	5.9	9.2	4.8
B[ghi]P	0.0	1578	2383	1279	1695	1875	812	1582	639	334	565	577	471	109	112	112	130	49	32	73	2.1	70	75	2.88	2.8	2.5	3.9	2.0

carbon numbers (iC_4 and arC_7). This trend is particularly notable at the temperature of 1350 °C (see Fig. 5d), suggesting rapid consumption of 2, 3 and 4 ring PAHs in soot particle growth at higher temperatures. The heptane tested, once again, departed from this general behaviour.

Considering Fig. 5 in its entirety, it can be seen that the concentrations of 4, 5 and 6 ring PAHs (especially Group B2 members) decreased when the temperature of the reactor was raised to from 1050 to 1350 °C. Finally, Fig. 5a and d show increasing and decreasing trends in total PAH concentrations with carbon number at 1050 and 1350 °C, respectively; however, Fig. 5b and c show no clear trend of influence of carbon number on the total PAH concentrations at the intermediate temperatures of 1150 °C and 1250 °C respectively.

One possible explanation for the increase in total PAH concentrations with increasing carbon number at 1050 °C is that the kinetics for the growth of PAHs to soot was slow, hence, PAHs continuously accumulate in comparatively high concentrations. This result is supported by the lower soot concentrations shown in Table 5 for all the hydrocarbons tested. At higher temperature of 1350 °C, the total PAH concentrations decreased with increasing carbon number since the rate of growth of PAHs to soot accelerated, exceeding the rate at which the PAHs were formed [16].

3.6. Toxicity of soot particles produced by C_1-C_7 hydrocarbons

This section examines the toxicity of soot particles generated from pyrolysis of the seven hydrocarbons. The weighted carcinogenicity of PAHs (WC-PAHs), was defined in [16] (see Eq.1) as the summation of the product of individual EPA16 priority PAH concentrations (C_i) and their corresponding toxicity equivalent factors (TEF). The TEFs selected are shown in Table 1 as proposed by Nisbet and Lagoy [32] and are widely used for assessing PAH toxicity.

$$\text{WC}-\text{PAHs} = \sum_{i=1}^{16} (TEF_i * Ci) \tag{1}$$

Fig. 6a and b show the WC-PAHs on volume of gas and soot mass bases respectively. It is apparent from Fig. 6a that soot particles produced from toluene (arC_7) pyrolysis produced the highest WC-PAHs at a temperature of 1050 °C. The WC-PAH of arC_7 on volume of gas basis at a temperature of 1050 °C was 3.5 times that of C_3, 4 times that of iC_4, 16 times that of nC_4 and 49 times that of the C_2 and nC_7 hydrocarbons. This result is not due to the high soot mass produced by toluene pyrolysis at 1050 °C, but due to the substantial concentrations of Group B2 PAHs (particularly B(a)P, D(a,h)A and B(k)F) generated from toluene soot particles. PAHs contributing to the toxicity of soot particles from the seven hydrocarbons are shown in Tables 7 and 8.

Fig. 6b shows that propane soot particles produced the highest WC – PAHs on soot mass basis at a temperature of 1050 °C, and there was a clear decreasing trend of carcinogenicity with temperature increase. The weighted carcinogenicity of propane soot particles (soot mass basis) at 1050 °C was 2.4 times that of arC_7, 3.3 times that of nC_7, 3.9 times that of n-C_4, 5.3 times that of C_2 and 13.2 times that of the iC_4 hydrocarbon. It is also apparent from Fig. 6b that the WC – PAHs decreased with increasing carbon number of the hydrocarbon at the temperature of 1150 °C.

It is interesting to note that the trend of the WC-PAHs in Fig. 6b, reflects that of soot particle number concentrations in Table 6. This analogy could mean that the carcinogenicity of soot particles is not only dependent on the mass of soot particles, but also on their number. Individual PAHs contributing to the WC – PAHs on soot mass basis are shown in Table 8. In Table 8, the contribution of Group D PAHs (low ring number and relatively low carcinogenicity factors) to the WC-PAHs stands out as being relatively small, either because those PAHs were not detected (nd) on the soot extracts or their concentrations on the soot particle was low. Group D PAHs have higher vapour pressure (0.0006–10.4 Pa at 25 °C) and lower boiling points (218–404 °C)

relative to Group B2, which may have reduced their condensation rates on the soot particles [16].

Closer inspection of Fig. 6a and b shows that aromatisation in the C_7 hydrocarbons increased the toxicity of soot particles at a temperature of 1050 °C, but the converse can be observed at the temperature range of 1150–1350 °C. Fig. 6a shows that the WC-PAH of iC_4 soot particles within temperatures of 1050–1150 °C is higher than those for nC_4, suggesting that isomerisation of the C_4 hydrocarbon is significant in contributing to the abundance of Group B2 PAHs. Again, as in the case of aromatisation of the C7 hydrocarbons, the opposite is true for the C_4 isomerised hydrocarbon when the temperature was increased from 1250 to 1350 °C. A potential implication of these observations is that hydrocarbons with higher carbon number, which are known to have higher cetane numbers and shorter ignition delays in compression ignition engines [47], produce substantial particulate mass, but the PAHs on the particulates are generally of lower toxicity. However, where diesel fuel ignition delays decrease, this can also reduce in-cylinder temperatures, which might be expected to increase the WC-PAHs in Fig. 6b.

4. Conclusions

The conclusions from the results reported can be summarised as follows:

1) Increasing carbon number of C_1–C_7 hydrocarbons was observed to increase their propensities to form soot particles in the effluent gas (nitrogen) especially at the initial temperature of 1050 °C (except for heptane which was observed to be outside this trend), and this effect of carbon number on soot concentration becomes much less apparent as the temperature of the reactor was raised from 1050 to 1350 °C.
2) Methane pyrolysis was observed to have the smallest number of primary soot particles at the temperature of 1050 °C when compared with most of the C_2–C_7 hydrocarbons. At the lowest temperature of 1050 °C, the particle average size for toluene (308 nm) was roughly similar to that produced at the highest temperature of 1350 °C by the C_1–C_7 aliphatic hydrocarbons.
3) Increasing the temperature of the reactor from 1050 to 1350 °C, decreased the total PAH concentrations regardless of the carbon number of the hydrocarbons investigated.
4) Increasing carbon number from C_1 to C_7 decreased the gas phase PAH concentration at the temperature of 1350 °C. Similarly, the particulate phase PAH concentration (including those of the Group B2 PAHs) decreased at a temperature of 1150 °C when the carbon number was increased from C_1 to C_7. No clear trends were observed at temperatures of 1050 and 1250 °C.
5) The total PAH concentrations tended to increase with increasing carbon number (excluding heptane) at the temperature of 1050 °C but an opposite (decreasing) trend was observed at 1350 °C.
6) Isomerisation in the C_4 hydrocarbons and aromatisation in the C_7 hydrocarbons increased substantially, the soot propensities, the abundance of particle phase PAHs and carcinogenicity on volume of gas basis at the temperature of 1050 °C.
7) Toluene and propane soot particles had the highest weighted carcinogenicities at the temperature of 1050 °C on gas volume and soot mass bases respectively. At the temperature of 1150 °C, the weighted carcinogenicity (soot mass basis) was observed to decrease with increasing carbon number of the hydrocarbon.

Acknowledgments

The first author wishes to gratefully acknowledge the Petroleum Technology Development Fund (PTDF) for sponsoring his research degree at University College London (UCL). The authors would also like to acknowledge the support of the UK Engineering and Physical Sciences Research Council (EPSRC) (grant number EP/M007960/2).

Appendix A

Table A1

Table A1
Particle mass measurements from DMS500 (μg/cm^3).

Temperature (°C)	1050	1150	1250	1350
Methane (C_1)	0.00001	0.43	2.55	3.04
Ethane (C_2)	0.048	0.75	1.95	2.53
Propane (C_3)	0.15	0.50	2.31	2.96
n-butane (nC_4)	0.11	1.02	2.39	3.45
i-butane (iC_4)	0.32	1.50	2.78	3.87
Heptane (nC_7)	0.03	0.98	1.78	2.00
Toluene (arC_7)	1.76	3.26	4.27	4.14

References

[1] H. Richter, J. Howard, Formation of polycyclic aromatic hydrocarbons and their growth to soot—a review of chemical reaction pathways, 26(4–6), 2000. doi: 10.1016/S0360-1285(00)00009-5.
[2] J.P. Longwell, The formation of polycyclic aromatic hydrocarbons by combustion, Nineteenth Symp (Intl) Combust. 1982:1339–50. doi.org/10.1016/S0082-0784(82)80310-X.
[3] Graham SC, Homer JB, Rosenfeld JLJ. The formation and coagulation of soot aerosols generated by the pyrolysis of aromatic hydrocarbons. Proc R Soc A Math Phys Eng Sci 1975;344(1637):259–85. http://dx.doi.org/10.1098/rspa.1975.0101.
[4] Kim K-H, Jahan SA, Kabir E, Brown RJC. A review of airborne polycyclic aromatic hydrocarbons (PAHs) and their human health effects. Environ Int 2013;60:71–80. http://dx.doi.org/10.1016/j.envint.2013.07.019.
[5] Richter H, Grieco WJ, Howard JB. Formation mechanism of polycyclic aromatic hydrocarbons and fullerenes in premixed benzene flames. Combust Flame 1999;119(1–2):1–22. http://dx.doi.org/10.1016/S0010-2180(99)00032-2.
[6] Shukla B, Koshi M. Comparative study on the growth mechanisms of PAHs. Combust Flame 2011;158(2):369–75. http://dx.doi.org/10.1016/j.combustflame.2010.09.012.
[7] D'Anna A, Violi A, D'Alessio A. Modeling the rich combustion of aliphatic hydrocarbons. Combust Flame 2000;121(3):418–29. http://dx.doi.org/10.1016/S0010-2180(99)00163-7.
[8] Frenklach M. Reaction mechanism of soot formation in flames. Phys Chem Chem Phys 2002;4(11):2028–37. http://dx.doi.org/10.1039/b110045a.
[9] Shukla B, Miyoshi A, Koshi M. Role of methyl radicals in the growth of PAHs. J Am Soc Mass Spectrom 2010;21(4):534–44. http://dx.doi.org/10.1016/j.jasms.2009.12.019.
[10] Shukla B, Susa A, Miyoshi A, Koshi M. Role of phenyl radicals in the growth of polycyclic aromatic hydrocarbons. J Phys Chem A 2008;112(11):2362–9. http://dx.doi.org/10.1021/jp7098398.
[11] Shukla B, Koshi M. A novel route for PAH growth in HACA based mechanisms. Combust Flame 2012;159(12):3589–96. http://dx.doi.org/10.1016/j.

combustflame.2012.08.007.
[12] Shukla B, Susa A, Miyoshi A, Koshi M. In Situ direct sampling mass spectrometric study on formation of polycyclic aromatic hydrocarbons in toluene pyrolysis. J Phys Chem A 2007;111(34):8308–24. http://dx.doi.org/10.1021/jp071813d.
[13] Wang R, Cadman P. Soot and PAH production from spray combustion of different hydrocarbons behind reflected shock waves. Combust Flame 1998;112:359–70. doi.org/10.1016/S0010-2180(97)00134-X.
[14] Bruinsma OSL, Moulijn JA. The pyrolytic formation of polycyclic aromatic hydrocarbons from benzene, toluene, ethylbenze, e, styrene, phenylacetylene and n-decane in relation to fossil fuels utilization. Fuel Process Technol 1988;18(3):213–36. http://dx.doi.org/10.1016/0378-3820(88)90048-3.
[15] Furuhata T, Kobayashi Y, Hayashida K, Arai M. Behavior of PAHs and PM in a diffusion flame of paraffin fuels. Fuel 2012;91(1):16–25. http://dx.doi.org/10.1016/j.fuel.2011.07.014.
[16] Dandajeh HA, Ladommatos N, Hellier P, Eveleigh A. Effects of unsaturation of C2 and C3 hydrocarbons on the formation of PAHs and on the toxicity of soot particles. Fuel 2017;194:306–20. http://dx.doi.org/10.1016/j.fuel.2017.01.015.
[17] Sharma RK, Hajaligol MR. Effect of pyrolysis conditions on the formation of polycyclic aromatic hydrocarbons (PAHs) from polyphenolic compounds. J Anal Appl Pyrolysis 2003;66(1–2):123–44. http://dx.doi.org/10.1016/S0165-2370(02)00109-2.
[18] Sánchez NE, Callejas a, Millera a, Bilbao R, Alzueta MU, Formation of PAH and soot during acetylene pyrolysis at different gas residence times and reaction temperatures, Energy, 43(1), 30–36, 2012. doi: 10.1016/j.energy.2011.12.009.
[19] Zhang Y, Yuan W, Cai J, Zhang L, Qi F, Li Y. Product identification and mass spectrometric analysis of n-butane and i-butane pyrolysis at low pressure. Chin J Chem Phys 2013;26(2):151. http://dx.doi.org/10.1063/1674-0068/26/02/151-156.
[20] Marinov NM, Castaldi MJ, Melius CF, Tsang W, Marinov NM, Castaldi MJ, et al. Aromatic and polycyclic aromatic hydrocarbon formation in a premixed propane flame aromatic and polycyclic aromatic hydrocarbon formation in a premixed propane flame 2016;2202. doi: 10.1080/00102209708935714.
[21] Zhang L, Cai J, Zhang T, Qi F. Kinetic modeling study of toluene pyrolysis at low pressure. Combust Flame 2010;157:1686–97. http://dx.doi.org/10.1016/j.combustflame.2010.04.002.
[22] Zhang T, Zhang L, Hong X, Zhang K, Qi F, Law CK, et al. An experimental and theoretical study of toluene pyrolysis with tunable synchrotron VUV photoionization and molecular-beam mass spectrometry. Combust Flame 2009;156:2071–83. http://dx.doi.org/10.1016/j.combustflame.2009.06.001.
[23] Botero ML, Chen D, González-Calera S, Jefferson D, Kraft M. HRTEM evaluation of soot particles produced by the non-premixed combustion of liquid fuels. Carbon N Y 2016;96:459–73. http://dx.doi.org/10.1016/j.carbon.2015.09.077.
[24] Marinov NM, Castaldi MJ, Melius CF, Tsang W. Aromatic and polycyclic aromatic hydrocarbon formation in a premixed propane flame. Combust Sci Technol 1997;128(1–6):295–342. http://dx.doi.org/10.1080/00102209708935714.
[25] Siegmann K, Sattler K. Formation mechanism for polycyclic aromatic hydrocarbons in methane flames. J Chem Phys 2000;112(2):698–709. http://dx.doi.org/10.1063/1.480648.
[26] El Bakali A, Mercier X, Wartel M, Acevedo F, Burns I, Gasnot L, et al. Modeling of PAHs in low pressure sooting premixed methane flame. Energy 2012;43:73–84. http://dx.doi.org/10.1016/j.energy.2011.12.026.
[27] Schenk M, Hansen N, Vieker H, Beyer A, Gölzhäuser A, Kohse-Höinghaus K. PAH formation and soot morphology in flames of C4 fuels. Proc Combust Inst 2015;35(2):1761–9. http://dx.doi.org/10.1016/j.proci.2014.06.139.
[28] Ladommatos N, Rubenstein P, Bennett P. Some effects of molecular structure of single hydrocarbons on sooting tendency. Fuel 1996;75(2):114–24. http://dx.doi.org/10.1016/0016-2361(94)00251-7.
[29] Crossley SP, Alvarez WE, Resasco DE, Novel micropyrolyis index (MPI) to estimate the sooting tendency of fuels, no. 6, pp. 2455–2464, 2008. doi: 10.1021/ef800058y.
[30] McEnally CS, Pfefferle LD. Sooting tendencies of oxygenated hydrocarbons in laboratory-scale flames. Environ Sci Technol 2011;45(6):2498–503. http://dx.doi.org/10.1021/es103733q.
[31] Schoeny R, Poirier K. Provisional guidance for quantitative risk assessment of polycyclic aromatic hydrocarbons. US Environmental Protection Agency, Office of Research and Development, Office of Health and Environmental Assessment, Washington DC (NTIS PB94116571); 1993. doi: EPA/600/R-93/089.
[32] Nisbet ICT, LaGoy PK. Toxic equivalency factors (TEFs) for polycyclic aromatic hydrocarbons (PAHs). Regul Toxicol Pharmacol 1992;16(3):290–300. http://dx.doi.org/10.1016/0273-2300(92)90009-X.
[33] EPA Method TO. Method TO-13A: Compendium of Methods for the Determination of Toxic Organic Compounds in Ambient Air Second Edition Compendium Method TO-13A Determination of Polycyclic Aromatic Hydrocarbons (PAHs) in Ambient Air Using Gas Chromatography/Mass Spectrom. EPA 1999.
[34] Environmental Protection Agency (EPA). Test Methods for evaluating solid waste. Method 3541 US EPA SW-846, 3rd ed. Update III; US GPO: Washington DC; 1995.
[35] Ruiz MP, Callejas A, Millera A, Alzueta MU, Bilbao R, Soot formation from C2H2 and C2H4 pyrolysis at different temperatures, J Anal Appl Pyrolysis, 79(1–2), SPEC. ISS., 244–251, 2007. doi: 10.1016/j.jaap.2006.10.012.
[36] Murphy DB. Analysis of products of high-temperature pyrolysis of various hydrocarbons. Carbon 1997;35:1819–23. doi.org/10.1016/S0008-6223(97), 00109-7.
[37] Guéret C, Daroux M, Billaud F. Methane pyrolysis: thermodynamics. Chem Eng Sci 1997;52(5):815–27. http://dx.doi.org/10.1016/S0009-2509(96)00444-7.
[38] Calcote HF, Manos DM. Effect of molecular structure on incipient soot formation. Combust Flame 1983;49(1–3):289–304. http://dx.doi.org/10.1016/0010-2180(83)90172-4.
[39] Oehlschlaeger MA, Davidson DF, Hanson RK. High-temperature thermal decomposition of isobutane and n-butane behind shock waves. J Phys Chem A 2004;108(19):4247–53. http://dx.doi.org/10.1021/jp0313627.
[40] Dandajeh HA, Effect of molecular structure of liquid and gaseous fuels on the formation and emission of PAHs and soot, PhD thesis, University College London, pp. 107–108, 2018.
[41] Kittelson D, Kraft M, Street P, Street P, Particle Formation and Models in internal Combustion Engines, Cambridge Centre for Computational Chemical Engineering. p. 4–6, 2014.
[42] Eveleigh A, The influence of fuel molecular structure on particulate emission investigated with isotope tracing, PhD thesis, University College London. pp. 57, 2015.
[43] Heywood JP. Internal combustion engine fundamentals. 1988. 1st Ed. New York: McGraw-Hill.
[44] Sánchez NE, Millera Á, Bilbao R, Alzueta MU. Polycyclic aromatic hydrocarbons (PAH), soot and light gases formed in the pyrolysis of acetylene at different temperatures: effect of fuel concentration. J Anal Appl Pyrolysis 2013;103:126–33. http://dx.doi.org/10.1016/j.jaap.2012.10.027.
[45] Aracil I, Font R, Conesa JA. Semivolatile and volatile compounds from the pyrolysis and combustion of polyvinyl chloride. J Anal Appl Pyrolysis 2005;74:465–78. http://dx.doi.org/10.1016/j.jaap.2004.09.008.
[46] Smith R. Formation of radicals and complex organic compounds by high-temperature pyrolysis: the pyrolysis of toluene. Combust Flame 1979;35:179–90. http://dx.doi.org/10.1016/0010-2180(79)90021-X.
[47] Koivisto E, Ladommatos N, Gold M. Systematic study of the effect of the hydroxyl functional group in alcohol molecules on compression ignition and exhaust gas emissions. Fuel 2015;153:650–63. http://dx.doi.org/10.1016/j.fuel.2015.03.042.